

FRAME-RATE REQUIREMENTS FOR DIGITAL FUNCTION GENERATION
IN HYBRID COMPUTING LOOPS

Robert M. Howe
The University of Michigan, Ann Arbor, Michigan

1. INTRODUCTION

By far the most prevalent use of digital computers in hybrid (combined analog-digital) computation is for function generation. This is particularly true for problems involving simulation of aerospace vehicles, where the aerodynamic forces and moments may be complex functions of three or more variables. Typically the required function generation will be done on the digital computer using table lookup and linear interpolation, and the rest of the computation, including integration, will be done on the analog computer.

Since the sample rate at which the digital computer can generate the nonlinear functions will be limited by the speed of the computer as well as the number and complexity of the required functions, it becomes important to understand the effect of this limitation on the overall dynamic accuracy of the hybrid solution. The purpose of this paper is to present quantitative estimates of these dynamic effects and the corresponding tradeoffs between computing speed and accuracy. Such considerations become important in estimating the capability of existing or proposed hybrid computer systems to solve large nonlinear simulation problems, and to estimate the performance improvement which can be obtained using specially-configured digital hardware dedicated to function generation.

2. FORMULATION OF THE PROBLEM TO BE ANALYZED

The type of nonlinear problem normally implemented on a hybrid computer is so large and complex that analytic techniques for dynamic error analysis cannot be applied directly. Fortunately, however, subsections of the problem can often be quasi-linearized without destroying the basic nature of the dynamic behavior of the system. The quasi-linear subsystem can then be analyzed using Z-transform theory to determine the effect of digital frame-rate on dynamic accuracy.⁽¹⁾ In particular, for aerospace vehicles it turns out that the most critical dynamic computing loops usually turn out to be second-order when linearized.

For example, the equation for angle of attack, x , turns out to be well-approximated by the following second-order differential equation:

$$\ddot{x} = -F(x, \dot{x}, y, w, \dots) + f(t) \quad (2.1)$$

where $f(t)$ is the input or forcing function and F is a nonlinear function not only of x and \dot{x} , but also other variables y, w, \dots (e.g., Mach number, altitude, etc.). If we assume that y, w, \dots vary slowly enough compared with angle of attack, x , then we can consider them constant for purposes of dynamic error analysis. We will further assume a small enough range in x so that the function F can be replaced approximately by a linear function in x and \dot{x} . Then we can write:

$$\ddot{x} = -(2\zeta a\dot{x} + a^2 x) + f(t) \quad (2.2)$$

which represents a simple linear second-order system with undamped natural frequency a and damping ratio ζ . Figure 2.1 shows a block diagram of the system, mechanized in hybrid form with analog (i.e., continuous) input $f(t)$, analog integrators, and digital generation of the function $2\zeta a\dot{x} + a^2 x$. In the figure the Laplace transform of the

continuous analog signals is also shown. The two switches in the figure represent, respectively, the conversion of the analog signals $y(t)$ and $x(t)$ to digital data sequences $\{y_n\}$ and $\{x_n\}$. This corresponds to A to D (analog to digital) conversion. In practice this is usually accomplished with a single A to D converter multiplexed between the channels, with sample-hold amplifiers on each channel to avoid time skew. The transforms of the time-domain data sequences $\{y_n\}$ and $\{x_n\}$, respectively, are the Z-transforms $Y^*(z)$ and $X^*(z)$.⁽¹⁾ In the digital computer these are combined with proper weighting factors to form the data sequence $\{c_n\}$ with a delay (frame time) T . This output data sequence $\{c_n\}$ is then converted to a continuous signal $c_e(t)$, using a DAC (digital-to-analog converter). This is shown as the mixed-data system in Figure 2.1. The DAC output $c_e(t)$ is updated every T seconds to the value represented by the next digital word in the data sequence $\{c_n\}$. This represents zero-order extrapolation.

3. DYNAMIC ERROR FOR SECOND-ORDER SYSTEM, NO UPDATING

The Z-transform of the output of the hybrid computing loop in Figure 2.1 can be obtained analytically.⁽¹⁾ The expression is given in Appendix A. The poles of this Z-transform can be related to the characteristic roots of the equivalent linear system, from which the following expressions are obtained for the natural frequency, \hat{a} , and the damping ratio, $\hat{\zeta}$, of the hybrid loop.

$$\text{nat. freq.} = \hat{a} = a \left[1 + \frac{9\zeta - 12\zeta^3}{4(1-\zeta^2)} aT + \dots \right] \quad (3.3)$$

$$\text{damping ratio} = \hat{\zeta} = \zeta - \left(\frac{3}{4} - 3\zeta^2 \right) aT + \dots \quad (3.4)$$

Thus the errors in frequency and damping due to the hybrid function generation vary as the first power of the dimensionless frame period, aT . Figure 3.1 shows the percentage error in actual frequency (not undamped natural frequency) and damping ratio error plotted against damping ratio ζ of the second order system. For example, assume $aT = 0.1$ (i.e., 10 samples per radian or 20π samples per cycle). For $\zeta = 0.2$ the frequency error is 2% (hybrid-loop frequency is 2% high) and the damping ratio error is -0.07 (damping ratio of the hybrid loop is 0.13 instead of 0.2). These are very sizeable dynamic errors, especially in the case of the damping ratio, and yet the digital computer is generating over 62 function samples per cycle of the second-order system transient! Even for $aT = 0.01$ (628 frames per cycle) the hybrid computing loop exhibits a damping ratio error of -0.0064 or 3.2%. For a one hertz oscillatory system this means a digital frame time of 1/628 seconds or about 1.6 milliseconds.

The above results are admittedly based on a quasi-linear analysis of a nonlinear problem, although experience has shown that it gives a good indication of the dynamic errors to be expected. The error in hybrid system transfer function for a sinusoidal input $f(t)$ can also be computed using Z-transform theory⁽¹⁾ and will vary as the first power of aT .

It should be noted that the nonlinear function F in Equation (2.1) can sometimes be computed as $F = xG(x, \dot{x}, y, w, \dots)$. Here G represents the slope of the F versus x function. If the digital computer is used to

calculate G and G is not strongly a function of x, then the dynamic picture can be much better than the above analysis has indicated. One cannot, however, count on being able to use this mechanization as a general approach.

4. DYNAMIC ERROR FOR SECOND-ORDER SYSTEM WITH UPDATING

It is interesting to note that the hybrid feedback loop in Figure 2.1 can be viewed as approximately equivalent to an analog transport delay of 1.5T. This is evident in Figure 4.1. This delay is the primary cause for the dynamic errors observed in the previous section. The delay can be eliminated to first order by driving each A to D converter with the continuous variable plus 1.5T times the time derivative of the variable. This has been done in the mechanization shown in Figure 4.2. The Z-transform of the output x(t) of this hybrid loop with updating can be obtained analytically and is given in Appendix B. From the poles of this Z-transform the following expressions are obtained for the equivalent natural frequency and damping ratio of the hybrid loop:

$$\text{nat. freq.} = \hat{\omega} = a \left[\frac{1 + \frac{13}{24} - \frac{41}{6} \zeta^2 + \frac{23}{3} \zeta^4}{1 - \zeta^2} (aT)^2 + \dots \right] \quad (4.1)$$

$$\text{damping ratio} = \hat{\zeta} = \zeta \left[1 + \left(3 - \frac{23}{3} \zeta^2 \right) (aT)^2 + \dots \right] \quad (4.2)$$

where a and ζ represent the ideal undamped natural frequency and damping ratio, respectively. Note in Equations (4.1) and (4.2) that the errors vary as $(aT)^2$ as opposed to (aT) in Equations (3.3) and (3.4) when no updating is used. This means that for a given dynamic accuracy requirement a much smaller number of samples per cycle is required when updating is used on the input variables to the digital function generator.

For example, we found in section 3 when no updating is used that for $\zeta = 0.2$ and $aT = 0.1$ (10 samples per radian) the hybrid-loop frequency is 2% high and the damping ratio is 0.13 instead of 0.2. When the updating shown in Figure 4.2 is used, the frequency is 0.27% low and the damping ratio is 0.205 instead of 0.2. Thus the improvement in hybrid-loop accuracy with updating is spectacular and a digital frame rate of 10 samples per radian (62.8 samples per cycle) gives quite good dynamic accuracy. Incidentally, for $(aT) = 0.1$, as in this example, the formulas in Equations (3.3) and (3.4) give quite accurate results when terms of order higher than $(aT)^2$ are neglected (for $\hat{\zeta} = 0.2$ within 0.013% in the $\hat{\omega}$ formula and 0.042% in the $\hat{\zeta}$ formula).

Another way to highlight the improvement which updating provides is to note that for the $\zeta = 0.2$ case it requires 117 samples per radian for the non-updating mechanization of Figure 2.1 (i.e., $aT = .0085$) to yield the same dynamic accuracy obtained with updating for 10 samples per radian ($aT = 0.1$).

The updating shown in Figure 4.2 assumes, of course, that the derivative of each of the function-generator input variables is available in analog form as well as the variables themselves. When this is not the case, two alternatives are possible. The first is to differentiate a variable using a bandwidth-limited differentiator circuit (i.e., a differentiator followed by a low-pass filter). The filter time-lag T_f is then added to the hybrid-loop lag of 1.5T in providing the updating. Thus, if \dot{x} is the analog approximation to the time derivative of x as obtained by such a circuit, then $x + (1.5T + T_f) \dot{x}$ becomes the input

to the A to D converter in the hybrid loop. The second alternative is to update the variable in the digital computer by performing a numerical approximation to the derivative. This has the disadvantage of tending to amplify the effects of A to D converter noise and can lead to instabilities for large frame times, aT .⁽²⁾

5. CONCLUSIONS

It has been shown in this paper that Z-transform theory can be used to predict the effect of digital function generation on the dynamics of a second-order hybrid computing loop. Such an analysis gives a good insight into the dynamic effect of digital function generation at a fixed frame rate on large nonlinear hybrid problems, such as aircraft or missile simulations. For the standard mechanization of hybrid computing loops it is concluded that approximately 100 digital frames per radian, i.e., 628 samples per cycle of the highest problem frequency involving digital function generation, is needed to keep dynamic errors below one percent.

If the analog variables to the digital computer are updated with rate information to compensate for the computational lags, only 5 to 10 samples per radian (31 to 62 samples per cycle) are needed for comparable (one percent) dynamic-error performance.

APPENDIX A

Z-Transform for Second-Order Hybrid Loop, No Updating

For the hybrid computing loop shown in Figure 2.1 (no updating of A to D input variables) the following formula is obtained for the Z transform of the output variable⁽³⁾

$X^*(z) =$

$$\frac{z(z-1)^2 \mathcal{Z} \left\{ \frac{1}{s} F(s) \right\} + 2\zeta a(z-1)^2 \left\{ s^{-1} H_e^*(z) \mathcal{Z} \left\{ \frac{1}{s} F(s) \right\} - s^{-2} H_e^*(z) \mathcal{Z} \left\{ \frac{1}{s} F(s) \right\} \right\}}{z^3 - 2z^2 + \left(1 + 2\zeta aT + \frac{a^2 T^2}{2} \right) z - 2\zeta aT + \frac{a^2 T^2}{2}} \quad (A.1)$$

Here $F(s)$ is the Laplace transform of the input function $f(t)$. The zeros of the denominator of this expression are in general complex and can be related to equivalent characteristic roots of a continuous linear system by the equations:

$$\sigma = \frac{1}{T} \ln |z_1|, \quad \omega = \frac{1}{T} \tan^{-1} \frac{z_{1i}}{z_{1r}} \quad (A.2)$$

where z_1 is one of the denominator roots and, when complex, is given by $z_1 = z_{1r} + jz_{1i}$; and where σ and ω are the real and imaginary parts of the equivalent characteristic roots for the continuous-system counterpart.

Since the denominator of Equation (A.1) is third order, it has three roots one of which must be real. It can be written in series form as⁽³⁾

$$Z_3 = 2\zeta aT + \left(4\zeta^2 - \frac{1}{2} \right) (aT)^2 + \dots \quad (A.3)$$

For $aT \ll 1$, which must always be the case for acceptable dynamic accuracy, $|z_3| \ll 1$ and, according to Equation (A.2), will lead to a rapidly decaying exponential transient.

The remaining two roots of the denominator approximately correspond to the ideal roots of an underdamped second order system and can be expressed as⁽³⁾

$$z_{1,2} = 1 - \zeta aT + \left(\frac{1}{4} - 2\zeta^2\right)(aT)^2 + \dots \pm jaT(\sqrt{1-\zeta^2} + \frac{5\zeta - 8\zeta^3}{4\sqrt{1-\zeta^2}}aT + \dots) \quad (\text{A. 4})$$

Applying Equation (A. 2) to these roots and noting that $\zeta = -\sigma/a$, and $\omega = a\sqrt{1-\zeta^2}$, we obtain Equations (3. 3) and (3. 4) as given earlier in the paper.

APPENDIX B

Z-Transform for Second-Order Hybrid Loop with Updating

For the hybrid computing loop with updating as shown in Figure 4. 2, it can be shown that the following formula is obtained for the z-transform of the output variable:

$$X^*(z) = \frac{N^*(z)}{z^4 - 2z^3 + (1 + 5\zeta aT + 2a^2 T^2)z^2 - (8\zeta aT + a^2 T^2)z + 3\zeta aT} \quad (\text{B. 1})$$

where we have not bothered to write out $N^*(z)$ because of its complexity. Two of the four roots of the denominator of Equation (B. 1) correspond approximately to the ideal roots of the underdamped second order system and are given by⁽³⁾

$$z_{1,2} = 1 - \zeta aT + (\zeta^2 - 0.5)(aT)^2 + (7\zeta^3 - 2.5\zeta)(aT)^3 + \dots \pm jaT\sqrt{1-\zeta^2} \left[1 - \zeta aT + \frac{375 - 6\zeta^2 + 7\zeta^4}{1-\zeta^2}(aT)^2 + \dots \right] \quad (\text{B. 2})$$

The remaining two roots can be written as⁽³⁾

$$z_{3,4} = \zeta aT + \left(\frac{1}{2} - \zeta^2\right)(aT)^2 \pm j\sqrt{3\zeta aT \left(1 + \frac{5}{3}\zeta aT + \dots\right)} \quad (\text{B. 3})$$

These are the two extraneous roots resulting from the hybrid feedback loop with updating. In deriving Equation (B. 1) it was assumed that the signal $y_i(t)$ in Figure 4. 2 is sampled just prior to the DAC update of $c_e(t)$ to its next value. Using Equations (A. 2) we obtain the following formulas for the decay constant, σ , and frequency, ω , associated with the extraneous roots z_3 and z_4 .

$$\sigma = \frac{1}{T} \ln |z_{1,2}| \cong \frac{1}{2T} \ln |3\zeta aT|, \quad aT \ll 1 \quad (\text{B. 4})$$

$$\omega = \frac{1}{T} \angle z_1 \cong \frac{1}{T} \tan^{-1} \frac{\sqrt{3\zeta aT}}{\zeta aT} \cong \frac{\pi}{2T}, \quad aT \ll 1 \quad (\text{B. 5})$$

Since the angular frequency associated with the hybrid sample period T is $2\pi/T$, reference to Equation (B. 5) shows that the extraneous pair of roots correspond to a frequency of approximately one-fourth the sample frequency. Equation (B. 4) shows that the transient is rapidly damped. Applying Equations (A. 2) to the principal roots given by Equation (B. 2) leads to Equations (4. 1) and (4. 2) as given earlier in the paper.

REFERENCES

1. Gilbert, E. G., "Dynamic Error Analysis of Digital and Combined Analog-Digital Computer Systems," *Simulation*, Vol. 6, No. 4, pp 241-257, April 1966.
2. Vichnevetsky, R., "Stability Contours for the Analysis of Analog/Digital Hybrid Simulation Loops," *Proc. SJCC*, pp 859-66, 1969.
3. Howe, R. M., and Fogarty, L. E., "Error Analysis of Computer Mechanization of Airframe Dynamics," Dept. of Aerospace Eng., Univ. of Michigan, Ann Arbor, Michigan revised report, Sept. 1975.

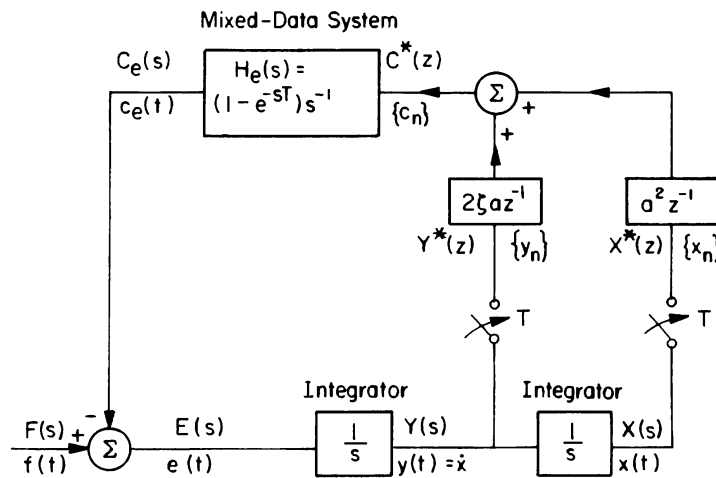


Figure 2. 1 Representation of the hybrid computing loop for solving the equation $\ddot{x} + 2\zeta a\dot{x} + a^2 x = f(t)$.

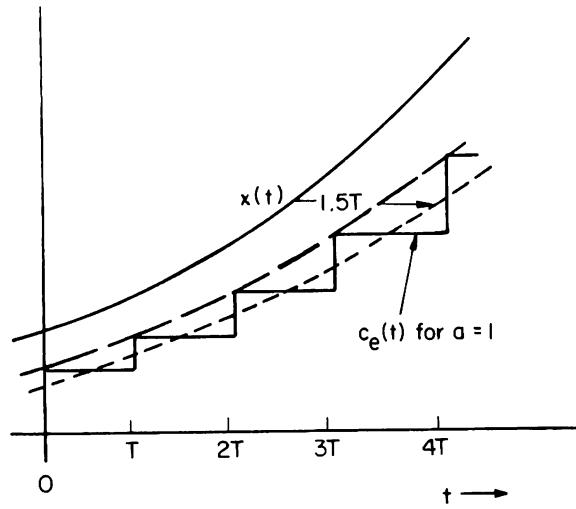


Figure 4.1 Transport delay of the hybrid feedback loop.

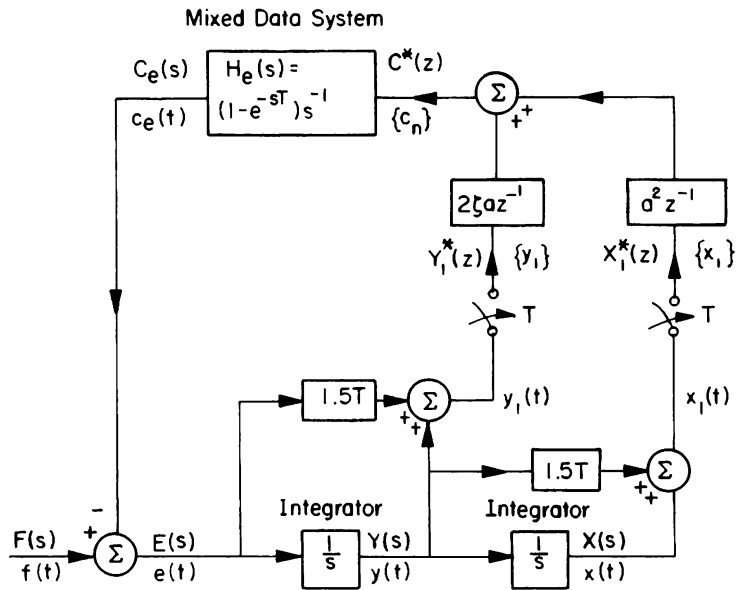


Figure 4.2 Hybrid computing loop with updating.

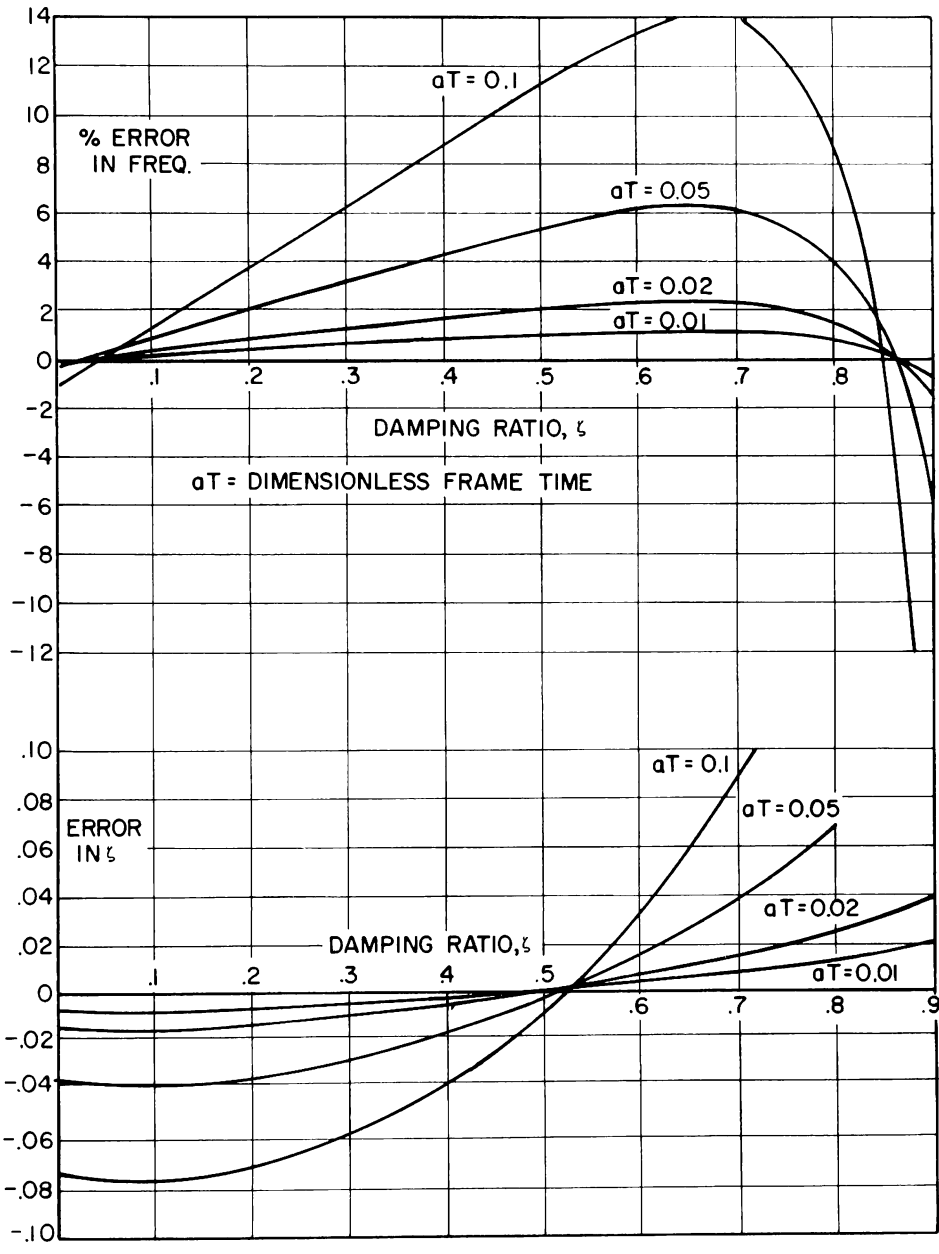


Figure 3.1